Atomic structures and the Mossbauer effect in amorphous La(Fe_xAl_{1-x})$_{13}$ alloys consisting of icosahedral clusters

1994 J. Phys.: Condens. Matter 6 3459

(http://iopscience.iop.org/0953-8984/6/19/001)

J. Phys.: Condens. Matter 6 (1994) 3459–3468. Printed in the UK

Atomic structures and the Mössbauer effect in amorphous $La(Fe_xAl_{1-x})_{13}$ alloys consisting of icosahedral clusters

T H Chiang†, E Matsubara‡, N Kataoka†, K Fukamichi† and Y Waseda§

† Department of Materials Science, Faculty of Engineering, Tohoku University, Sendai 980, Japan

‡ Department of Metallurgy, Faculty of Engineering, Kyoto University, Kyoto 606, Japan

§ Institute for Advanced Materials Processing, Tohoku University, Sendai 980, Japan

Received 24 November 1993

Abstract. Atomic structures of amorphous $La(Fe_xAl_{1-x})_{13}$ alloys (x = 0.80, 0.85, 0.90 and 0.95) were studied by x-ray diffraction. The distance between the icosahedral cluster and the La atom is slightly reduced with the increase in x. This indicates a slight change in arrangements of the icosahedral clusters around the La atom without changing the basic structure of the icosahedral clusters. On the other hand, the concentration dependence of coordination numbers for Fe–Fe pairs in the amorphous state resembles that in the crystalline state. From the ^{57}Fe Mössbauer spectra, it was revealed that local environment around Fe atoms in the $La(Fe_{0.9}Al_{0.1})_{13}$ alloy is very similar to that in the crystalline counterpart. The magnetic properties of the amorphous and crystalline alloys have been closely correlated with their characteristic atomic structures.

1. Introduction

The $La(Fe_xAl_{1-x})_{13}$ compounds with a cubic $NaZn_{13}$-type structure have been produced in a wide x range ($0.46 \leqslant x \leqslant 0.92$) (van der Kraan *et al* 1983) in spite of the positive mixing enthalpy for the La–Fe system (Kubaschewski 1982). The $La(Fe_xAl_{1-x})_{13}$ crystals show three different magnetic orders. The temperature dependence of the AC susceptibility curve exhibits a cusp in the low-Fe-concentration range ($0.46 \leqslant x \leqslant 0.62$), indicating a micromagnetic-like state. A ferromagnetic state appears on increasing the Fe concentration from 0.62 to 0.86. For higher Fe concentrations up to 0.92, the antiferromagnetic state becomes stable and a metamagnetic transition is induced by an external field of a few teslas (Palstra *et al* 1984). The ferromagnetic state is transformed into the antiferromagnetic state by applying a hydrostatic pressure (Abd-Elmeguid *et al* 1987). These magnetic properties are attributed to their characteristic atomic structure consisting of Fe(Al) icosahedral clusters located at the corner and a La atom at the body centre of a cubic cell (Helmholdt *et al* 1986).

Recently, the magnetic properties of amorphous $La(Fe_xAl_{1-x})_{13}$ alloys ($0.80 \leqslant x \leqslant 0.95$) have been investigated (Chiang *et al* 1991). The ferromagnetic state becomes unstable on increase in x, and re-entrant spin-glass behaviour is observed in the range where the crystals are antiferromagnetic. The $La(Fe_xAl_{1-x})_{13}$ alloys in the amorphous and crystalline states exhibit marked thermal expansion and elastic anomalies (Palstra *et al* 1985, Chiang *et al* 1992). It has been found that the Curie temperature of the amorphous alloys is higher than the Curie or Néel temperature of the crystals, which is in striking contrast with many other amorphous Fe-based alloys, because the ferromagnetism of almost all Fe-based alloys is much weaker in the amorphous state than in the crystalline state (Fukamichi *et al* 1989).

0953-8984/94/193459+10$19.50

The magnetic moment and the Curie temperature of Fe-based amorphous alloys are strongly affected by the atomic distance and coordination number of the nearest-neighbour Fe–Fe pairs. Thus, in the present study, the atomic structures of amorphous $La(Fe_xAl_{1-x})_{13}$ alloys ($0.80 \leqslant x \leqslant 0.95$) have been systematically investigated by x-ray diffraction. Furthermore, Mössbauer spectroscopy is sensitive to local physical properties. In particular, the local symmetry around an Fe atom in amorphous alloys can be determined through the interaction between the nuclear quadrupole moment and the electric field gradient created by the electric charges distributed around the Fe nucleus. It is useful, therefore, in shedding some light on the local atomic arrangement in the amorphous alloys. From the atomic distances and coordination numbers determined in the present work, the relationship between the atomic structures and magnetic properties of these amorphous alloys will be discussed.

2. Experimental details

Amorphous $La(Fe_xAl_{1-x})_{13}$ alloys about 0.3 mm thick were grown on a water-cooled Cu substrate by high-rate DC sputtering using alloy targets about 50 mm in diameter prepared by arc melting in an argon atmosphere. The argon gas pressure during sputtering was 40 mTorr. The target voltage and the anode current were 1.0 kV and 6.0 A, respectively. After the Cu substrate had been dissolved in a mixed solution of CrO_3 (500 g), H_2SO_4 (25 ml) and H_2O (1000 ml) at 350 K, the densities of the amorphous $La(Fe_xAl_{1-x})_{13}$ alloys were determined by the Archimedean method using toluene as a working fluid. Their densities are 6.67, 6.88, 7.11 and 7.31 Mg m^3 for $x = 0.80$, 0.85, 0.90 and 0.95, respectively.

The sputtered samples for x-ray diffraction measurement were cut into 10 mm by 20 mm plate with the Cu substrate. The sample surface was carefully polished with emery paper and 1 μm diamond paste in order to make the surface flat. The sample was kept in dry helium gas during measurement. The x-ray diffraction measurement was carried out, using the ordinary θ–2θ coupling geometry with a molybdenum x-ray target and a flat Ge(111) single-crystal monochromator in the incident beam. The scattering intensity from the sample was measured using a scintillation counter with a pulse height analyser in order to eliminate Fe and La fluorescent radiations.

The observed intensities were corrected for air scattering, absorption and polarization and converted to absolute units per atom by the generalized Krogh–Moe–Norman method (Wagner *et al* 1965) with the x-ray atomic scattering factors (*International Tables for X-ray Crystallography* vol IV 1974) including the anomalous dispersion terms (*International Tables for X-ray Crystallography* vol IV 1974). Then, the coherent intensity $I_{eu}(Q)$ in absolute units was obtained by subtracting the theoretical Compton scattering (*International Tables for X-ray Crystallography* vol III 1968) with the Breit–Dirac recoil factors. From the intensity $I_{eu}(Q)$, the reduced interference function $Qi(Q)$ of the sample was evaluated using the following equation (Waseda 1980):

$$Qi(Q) = \left(I_{eu}(Q) - \sum_{j=1}^{N} c_j f_j^2\right) \Big/ \left(\sum_{j=1}^{N} c_j f_j\right)^2 \tag{1}$$

where $Q = (4\pi \sin\theta)/\lambda$, θ is half the angle between the incident and the diffracted beam, λ is the wavelength, N is the total number of the constituent elements, and c_j and f_j are the atomic fraction and atomic scattering factor, respectively, of the jth element. The

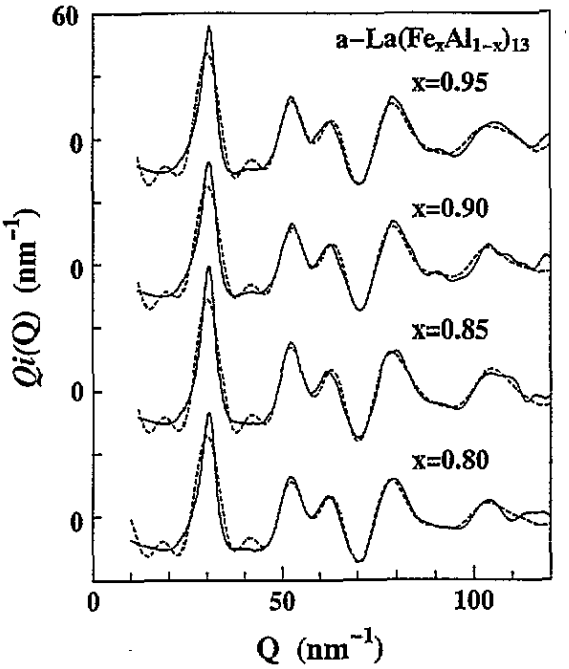

Figure 1. Interference functions $Qi(Q)$ of amorphous La(Fe$_x$Al$_{1-x}$)$_{13}$ alloys.

reduced radial distribution function (RDF) is calculated from the Fourier transformation of the interference functions:

$$2\pi^2 r\rho(r) = 2\pi^2 r\rho_0 + \int_0^{Q_{max}} Qi(Q)\sin(Qr)\,dQ \tag{2}$$

where $\rho(r)$ is the radial number density function and ρ_0 is the average number density of the sample.

The Mössbauer spectra were also measured at 290 K in the transition arrangement using a conventional constant-acceleration spectrometer with a ^{57}Co(Rh) source. The film samples were sputter deposited on polyimide substrates. The velocity calibration was made with an Fe foil at 290 K.

The magnetization measurement was carried out with a SQUID magnetometer. The differential magnetic susceptibility was calculated numerically from the adjoining two points of magnetization curves measured at each temperature in various magnetic fields.

3. Results and discussion

The interference functions $Qi(Q)$ of the amorphous La(Fe$_x$Al$_{1-x}$)$_{13}$ alloys ($0.80 \leqslant x \leqslant 0.95$) are shown in figure 1. The essential features in the structural profile are classified into the typical amorphous materials except for fairly distinct oscillations present even in the high-Q region. This kind of intensity profile is hardly observed in metallic amorphous alloys and rather resembles those for oxide glasses. Such a profile implies the presence of chemical short-range ordering clusters with definite bond lengths and angular relations (Egelstaff *et al* 1971).

The atomic distances and coordination numbers of these amorphous alloys were evaluated using the least-squares variational method for the interference function on the basis of the successful result applied to determining the local unit structure in SiO_2 and BeF_2 glasses (Narten and Levy 1969). The non-linear least-squares program developed by Levy *et al* (1966) was slightly modified and used in the present analysis. A brief summary of this method required for the following discussion will be given below.

The interference function $Qi(Q)$ may be given by (Narten and Levy 1969)

$$Qi(Q) = \sum_{j=1}^{N}\sum_{k=1}^{N'} c_j \frac{N_{jk}}{r_{jk}} \exp(-b_{jk}Q^2)\frac{f_j(Q)f_k(Q)}{\langle f\rangle^2}\sin(Qr_{jk}) + \sum_{l=1}^{N}\sum_{m=1}^{N} 4\pi\rho_0 c_l c_m \exp(-b_{lm}Q^2)\frac{f_l(Q)f_m(Q)}{\langle f\rangle^2}\frac{Qr_{lm}\cos(Qr_{lm}) - \sin(Qr_{lm})}{Q^2} \tag{3}$$

where N' is the number of near-neighbour atoms for a type-j atom, and N_{jk} and r_{jk} are the coordination number and the average distance of the j–k pairs. The value of b_{jk} is the mean square variation. The quantities r_{lm} and b_{lm}, respectively, represent the average size and the variation in the boundary region. In practice, the distances and coordination numbers of near-neighbour correlations are obtained by the least-squares calculation of equation (3) so as to reproduce the experimental interference function data. The interference functions obtained in this procedure are also shown by the broken curves in figure 1.

The starting parameters for the least-squares variations were set by calculating the average coordination numbers and atomic distances of the $La(Fe_{0.91}Al_{0.09})_{13}$ crystal at 300 K (Helmholdt *et al* 1986). These values are given in table 1 with the final results for each sample. The errors of the results were estimated from the variance–covariance matrix in the least-squares variational method. For the present least-squares variational analysis, it is assumed that Fe and Al atoms randomly share the atomic sites at the vertices of the icosahedral clusters in the amorphous structure as in the crystal structure. Since Fe and Al atoms randomly share the same atomic sites in the crystal structure (Helmholdt *et al* 1986), the coordination numbers for Fe–Al pairs are readily calculated simply by multiplying the ratio $(1-x)/x$ of the atomic fractions of Al and Fe by the coordination number for Fe–Fe pairs in table 1. In crystalline $La(Fe_{0.91}Al_{0.09})_{13}$ the icosahedral clusters formed by Fe and Al atoms located at their vertices and Fe atoms located at the centre are present at the corner of the cubic cell and the La atom is located at its body-centred position. Since the coordination numbers and atomic distances of Fe–Fe pairs for the amorphous alloys and for the crystal in table 1 show little difference, it is plausible that the local short-range ordering clusters in the amorphous alloys are the same icosahedral clusters as those in the crystalline state (Matsubara *et al* 1992).

The coordination numbers of the nearest-neighbour La–Fe pairs will provide us with structural information on the configuration around the icosahedral clusters around the La atom. That is, the coordination numbers of La–Fe pairs for the amorphous alloys are smaller than those for the crystals. These experimental results indicate that the distribution of the icosahedral clusters around the La atom in the amorphous alloy is extremely different from that in the crystal. Thus, the structure of the present amorphous alloys is not considered simply to be an assembly of microcrystals of $La(Fe_xAl_{1-x})_{13}$ (Cargill 1975). From the ratio of the coordination numbers for La–Fe(Al) pairs in the amorphous and crystalline alloys,

it is found that the number of the clusters around the La atom decreases to about three quarters of that in the crystals. This number decreases with increase in x.

The reduced RDFs for the amorphous La(Fe$_x$Al$_{1-x}$)$_{13}$ alloys are shown in figure 2. The solid and broken curves were obtained by the Fourier transformation of the experimental and calculated interference functions, respectively, in figure 1. The first peak composed of two peaks at about 0.25 and 0.32 nm is isolated from other peaks and fairly distinct oscillations are present even up to the middle distance range. These features also indicate the presence of the short-range ordering clusters in the present amorphous alloys.

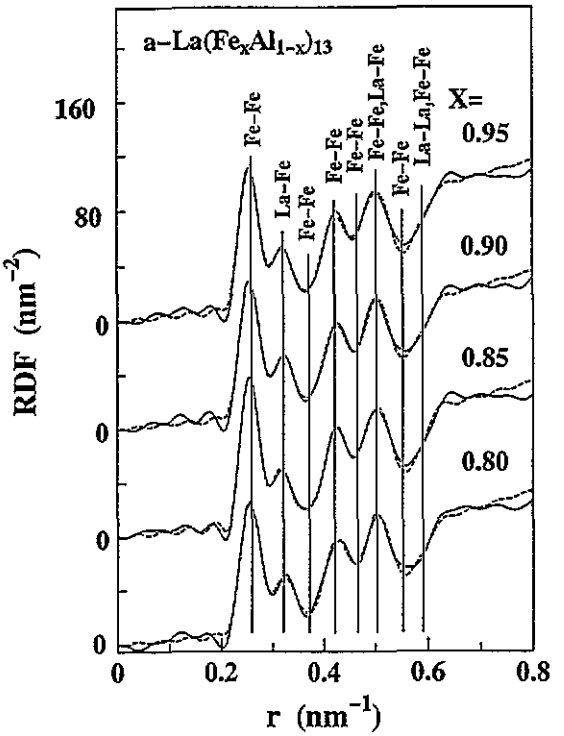

Figure 2. Concentration dependence of the RDFs of amorphous La(Fe$_x$Al$_{1-x}$)$_{13}$ alloys.

Fe atoms occupy two different sites in the La(Fe$_x$Al$_{1-x}$)$_{13}$ crystals, i.e. they are located at the centre and vertices of the icosahedron. The shortest Fe–Fe distance in the crystal is the distance between the Fe atoms at the centre and vertices. This distance is about 4% shorter than those between the Fe atoms at the vertices. Although the result of the least-squares variational analysis for the amorphous alloy clearly suggests the presence of icosahedral clusters, the structural parameters determined in the present analysis are the average values for all Fe atoms in the icosahedral cluster. Thus. the parameters of the amorphous alloys are compared with the average values calculated from the crystalline data summarized in the same table. The distance of the nearest-neighbour Fe–Fe pair hardly depends on the concentration, being about 0.255 nm ($0.80 \leqslant x \leqslant 0.95$). This value coincides with the Fe–Fe distance of the corresponding crystal.

Figure 3 shows the concentration dependence of the coordination number of the nearest-neighbour Fe–Fe pairs, together with that of the crystals (Palstra *et al* 1985). The value

Table 1. The coordination numbers and the atomic distances for amorphous $La(Fe_xAl_{1-x})_{13}$ alloys together with those for crystalline $La(Fe_{0.91}Al_{0.09})_{13}$.

			a-$La(Fe_xAl_{1-x})$							
	c-$La(Fe_{0.91}Al_{0.09})_{13}$		$x = 0.95$		$x = 0.90$		$x = 0.85$		$x = 0.80$	
	r (nm)	N	r (nm)	N	r (nm)	N	r (nm)	N	r (nm)	N
Fe–Fe	0.254	9.3	0.255 ± 0.002	9.5 ± 0.2	0.255 ± 0.002	9.2 ± 0.2	0.254 ± 0.002	8.3 ± 0.2	0.255 ± 0.002	8.4 ± 0.2
La–Fe	0.339	24.0	0.318 ± 0.002	17.2 ± 0.7	0.320 ± 0.002	17.8 ± 0.6	0.313 ± 0.002	18.2 ± 0.6	0.322 ± 0.002	19.0 ± 0.6
Fe–Fe	0.352	0.8	0.369 ± 0.006	1.1 ± 0.3	0.373 ± 0.005	1.2 ± 0.3	0.370 ± 0.007	0.6 ± 0.3	0.377 ± 0.005	0.7 ± 0.2
Fe–Fe	0.419	12.6	0.419 ± 0.002	10.8 ± 0.3	0.419 ± 0.002	10.5 ± 0.3	0.420 ± 0.002	10.8 ± 0.3	0.420 ± 0.002	10.5 ± 0.3
Fe–Fe	0.464	6.7	0.467 ± 0.002	7.3 ± 0.3	0.464 ± 0.002	6.5 ± 0.3	0.464 ± 0.002	6.6 ± 0.3	0.464 ± 0.002	6.9 ± 0.3
Fe–Fe	0.501	7.6	0.497 ± 0.002	7.7 ± 0.3	0.501 ± 0.002	7.6 ± 0.3	0.500 ± 0.002	7.1 ± 0.3	0.500 ± 0.002	7.5 ± 0.3
La–Fe	0.510	32.0	0.516 ± 0.002	26.9 ± 0.9	0.510 ± 0.002	26.1 ± 0.8	0.511 ± 0.002	27.1 ± 0.8	0.513 ± 0.002	26.4 ± 0.7
Fe–Fe	0.545	3.4	0.551 ± 0.002	4.8 ± 0.4	0.551 ± 0.002	4.7 ± 0.4	0.547 ± 0.002	4.2 ± 0.4	0.549 ± 0.002	4.3 ± 0.4
La–La	0.579	6.0	0.571 ± 0.003	5.2 ± 0.7	0.556 ± 0.002	5.2 ± 0.7	0.555 ± 0.002	5.2 ± 0.7	0.556 ± 0.002	5.2 ± 0.7
Fe–Fe	0.584	7.2	0.594 ± 0.002	6.6 ± 0.4	0.591 ± 0.002	7.8 ± 0.4	0.595 ± 0.002	7.3 ± 0.4	0.590 ± 0.002	7.1 ± 0.4

increases from 8.4 for $x = 0.8$ to 9.5 for $x = 0.95$ as seen from figure and the crystals take almost same values. Thus, the change in the coordination numbers of the nearest-neighbour Fe–Fe pairs in these amorphous alloys may be attributed not to any change in the internal structure of the icosahedral clusters but to an increase in the Fe concentration.

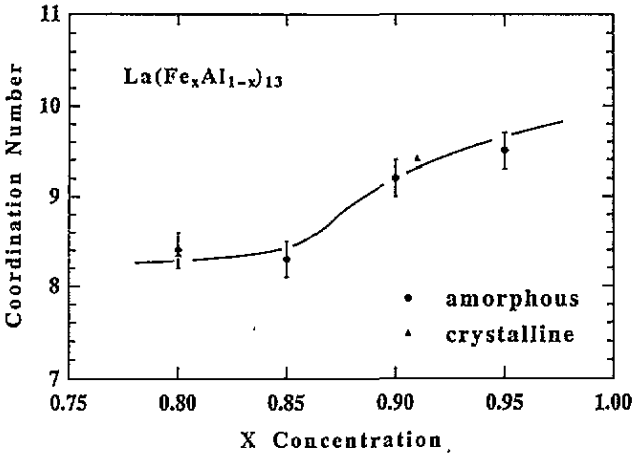

Figure 3. Concentration dependence of the coordination number of the nearest-neighbour Fe–Fe pairs in the amorphous state, together with that in the crystalline state (Palstra *et al* 1985).

The coordination number of La–Fe(Al) pairs is smaller in the amorphous state than in the crystalline state, and the atomic distance between the La–Fe(Al) nearest-neighbour pairs is shorter in the amorphous state than in the crystalline state. The La atom is totally surrounded by eight icosahedra, i.e. 24 Fe atoms. Thus, by dividing the coordination number of the La–Fe pairs in table 1 by 3, it is found that the La atom is surrounded by about six icosahedral clusters. The average radius of the La atom in the amorphous alloys calculated from the nearest-neighbour Fe–Fe and La–Fe pairs in table 1 is about 0.192 nm. Since the icosahedral clusters in the amorphous alloy resemble those in the crystal, the radius of the icosahedral cluster in the amorphous alloy is calculated to be 0.289 nm from the lattice parameter of the crystal (0.577 nm) by assuming a sphere for the icosahedral cluster. The ratio of the radius of the La atom to that of the icosahedral cluster in the amorphous alloy is 0.665. These experimental results suggest that the La atom is located at the octahedral site formed by the icosahedral cluster. Consequently, it is clearly seen that the atomic structure of the amorphous alloy is in striking contrast with that in the crystal, although the local structural unit is the icosahedral clusters of Fe(Al) atoms.

The ^{57}Fe Mössbauer spectra in the paramagnetic state were measured so as to discuss the local environment around Fe in La(Fe$_x$Al$_{1-x}$)$_{13}$ alloys. The Mössbauer spectra at 290 K for the amorphous and crystalline La(Fe$_{0.9}$Al$_{0.1}$)$_{13}$ alloys are shown in figure 4. The linewidth of the Mössbauer spectra is much wider than the natural linewidth of ^{57}Fe, which is ascribed to the distribution of the quadrupole interactions. The lower-velocity absorption peak is slightly larger than the higher-velocity peak. This asymmetric spectrum is attributed to the distribution of isomer shifts which correlates with the distribution of the quadrupole interactions. The average isomer shift and quadrupole splitting of the amorphous and crystalline alloys La(Fe$_{0.9}$Al$_{0.1}$)$_{13}$ are summarized in table 2, together with those of amorphous La$_{17.5}$Fe$_{82.5}$ alloy for comparison. These two values are equal in the amorphous

and crystalline states for the $La(Fe_{0.9}Al_{0.1})_{13}$. This implies that the local environment around the Fe atoms in two states is very similar to each other. This is consistent with the results obtained by x-ray diffraction. Furthermore, the value of average quadrupole splitting of the binary amorphous $La_{17.5}Fe_{82.5}$ alloy (Wakabayashi *et al* 1989) is slightly larger than that of the $La(Fe_{0.9}Al_{0.1})_{13}$ alloy, although the Fe content in both alloys is not so different. This suggests that there is some difference between the local atomic arrangements of the amorphous $La(Fe_{0.9}Al_{0.1})_{13}$ and $La_{17.5}Fe_{82.5}$ alloys. In the former amorphous alloy, the presence of icosahedral clusters may suppress the fluctuation in the local atomic arrangements such as the number of the nearest-neighbour atoms and the atomic distance.

Table 2. Mössbauer parameters at 290 K for amorphous and crystalline $La(Fe_{0.9}Al_{0.1})_{13}$ alloys, together with those of amorphous $La_{17.5}Fe_{82.5}$ alloy (Wakabayashi *et al* 1989).

Alloy	Average isomer shift (mm s^{-1})	Average quadrupole splitting (mm s^{-1})
c-$La(Fe_{0.9}Al_{0.1})_{13}$	−0.04	−0.39
a-$La(Fe_{0.9}Al_{0.1})_{13}$	−0.04	−0.39
a-$La_{17.5}Fe_{82.5}$	−0.06	−0.44

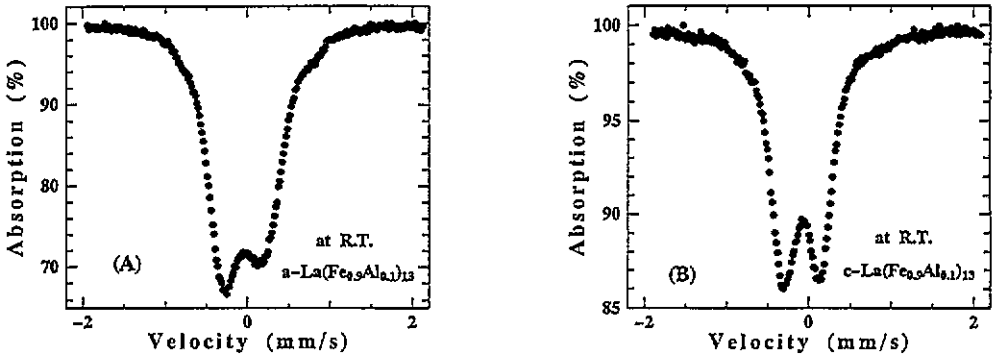

Figure 4. Mössbauer spectra at 290 K for $La(Fe_{0.9}Al_{0.1})_{13}$ alloys in (a) the amorphous state and (b) the crystalline state.

The magnetic moment and the Curie temperature of Fe-based alloys are strongly affected by the local environment of the Fe atoms characterized by the coordination number and the atomic distance of Fe–Fe nearest-neighbour pairs. According to the expanded finite-temperature theory taking into account the structural disorder, the magnetic moment of the central Fe atom depends on the number n of pairs defined by the central atom and the near-neighbour atoms located at a distance shorter than the average nearest-neighbour distance (Kakehashi 1990, 1991). That is, the Fe atom has a large moment of $2.5\mu_B$ for $n = 0$ and ferromagnetically interacts with the neighbouring atoms. For $n = 6$, the Fe atom has a small moment of $1.2\mu_B$ and interacts antiferromagnetically with the neighbouring atoms. The central Fe atom with $n = 12$ has no local moment (Kakehashi 1990). Thus, the antiferromagnetic interactions in the Fe-rich region might be ascribed

to large Fe–Fe coordination numbers, such as 12 and 10 for the Fe atom at the centre and vertices, respectively, of the icosahedral clusters. Furthermore, according to the relation between the magnetic state and the atomic distance for Fe (Wassermann 1990), the short distance of the nearest-neighbour Fe–Fe pair given in table 1 also introduces the antiferromagnetic interactions. However, the long-range antiferromagnetic order is not so feasible in amorphous alloys (Kaneyoshi 1984). As a result, it is expected that the spin-glass state due to the frustrated antiferromagnetic interactions exist at sufficiently low temperatures (Chiang *et al* 1991) in the concentration range where the antiferromagnetic order appears in the crystalline state. The increase in the spin freezing temperature with increasing x may be related to the increase in the coordination number from 8.4 for $x = 0.8$, to 9.5 for $x = 0.95$.

The magnetic properties of amorphous Fe-based alloys which exhibit spin-glass behaviour are very sensitive to the applied magnetic field and hydrostatic pressure (Goto *et al* 1988). Figure 5 shows the magnetic phase diagram of amorphous La(Fe$_{0.95}$Al$_{0.05}$)$_{13}$ alloy in the magnetic field, which is obtained from the differential magnetic susceptibility measurement. The Curie temperature T_C slightly increases with increase in the applied magnetic field. On the contrary, the freezing temperature of the transverse component of spins T_g and that of the longitudinal component T_f drastically decrease in a similar manner as obtained for the amorphous Fe–Y alloy system (Fujita *et al* 1993).

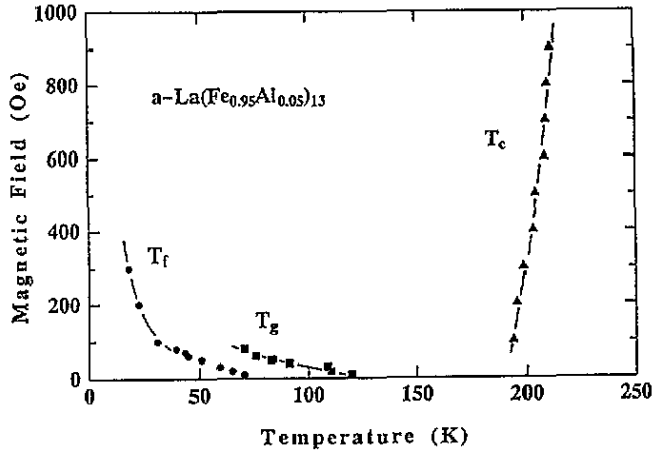

Figure 5. Magnetic phase diagram of an amorphous La(Fe$_{0.95}$Al$_{0.05}$)$_{13}$ alloy in the magnetic field.

4. Conclusions

The coordination numbers and atomic distances of Fe–Fe pairs in the amorphous La(Fe$_{0.9}$Al$_{0.1}$)$_{13}$ alloy are scarcely different from those in the corresponding crystalline alloy. The concentration dependence of the coordination numbers for Fe–Fe pairs in the amorphous state is analogous to that in the crystalline state. Similarity of the local environments around Fe atoms in both states is also confirmed by the Mössbauer effect measurements. The close relationship between the local structure and magnetic properties has been well appreciated.

Acknowledgment

The present work has been supported by Grant-in-Aid for Scientific Research (A)04402045 from the Japanese Ministry of Education, Science and Culture.

References

Abd-Elmeguid M M, Schleede B, Micklitz H, Palstra T T, Nieuwenhuys G J and Buschow K H J 1987 *Solid State Commun.* **63** 177–80
Cargill G S 1975 *Solid State Phys.* **30** 227–320
Chiang T H, Fukamichi K and Goto T 1992 *J. Phys.: Condens. Matter* **4** 7489–98
Chiang T H, Fukamichi K, Komatsu H and Goto T 1991 *J. Phys.: Condens. Matter* **3** 4045–55
Egelstaff P A, Page D I and Powles J G 1971 *Mod. Phys.* **20** 881–94
Fujita A, Komatsu H, Fukamichi K and Goto T 1993 *J. Phys.: Condens. Matter* **5** 3003–10
Fukamichi K, Goto T, Komastu H and Wakabayashi H 1989 *Proc. 4th Int. Conf. on Physics of Magnetic Materials* ed W Gorkowski, H K Lachowicz and H Szymczak (Singapore: World Scientific) pp 354–81
Goto T, Murayama C, Mori N, Wakabayashi H K, Fukamichi F and Komatsu H 1988 *J. Physique Coll.* **C8** 1143–4
Helmholdt R B, Palstra T T M, Nieuwenhuys G J, Mydosh J A, van der Kraan A M and Buschow K H J 1986 *Phys. Rev.* B **34** 169–73
1968 *International Tables for X-ray Crystallography* vol III (Birmingham: Kynoch) p 250
1974 *International Tables for X-ray Crystallography* vol IV (Birmingham: Kynoch) p 99
Kakehashi Y 1990 *Phys. Rev.* B **41** 9207–20
—— 1991 *Phys. Rev.* B **43** 10 820–31
Kaneyoshi T 1984 *Amorphous Mechanism* (Boca Raton, FL: CRC Press)
Kubaschewski O 1982 *Iron-Binary Phase Diagrams* (Berlin: Springer) pp 57–9D
Levy H A, Danford M D and Narten A H 1966 *Oak Ridge National Laboratories Report* ORNL-3960
Matsubara E, Waseda Y, Chiang T H and Fukamichi K 1992 *Mater. Trans. Japan Inst. Met.* **33** 155–7
Narten A H and Levy H A 1969 *Science* **165** 447–54
Palstra T T M, Nieuwenhuys G J, Mydosh J A and Buschow K H J 1985 *Phys. Rev.* B **31** 4622–32
Palstra T T M, Werij H G C, Nieuwenhuys G J, Mydosh J A, de Boer F R and Buschow K H J 1984 *J. Phys. F: Met. Phys.* **14** 1961–6
van der Kraan A M, Buschow K H J and Palstra T T M 1983 *Hyperfine Interact.* **15–6** 717–20
Wagner C N J, Ocken H and Joshi M L 1965 *Z. Naturf.* a **20** 325–35
Wakabayashi H, Goto T, Fukamichi K, Komatsu H, Morimoto S and Ito A 1989 *J. Phys. Soc. Japan* **58** 3383–91
Waseda Y 1980 *The Structure of Non-Crystalline Materials* (New York: McGraw-Hill) pp 27–51
Wassermann E F 1990 *Ferromagnetic Materials* vol 5 (Amsterdam: North-Holland) pp 237–322